

## The Wirewalker: A Vertically Profiling Instrument Carrier Powered by Ocean Waves

R. PINKEL, M. A. GOLDIN, J. A. SMITH, O. M. SUN, A. A. AJA, M. N. BUI, AND T. HUGHEN

*Marine Physical Laboratory, Scripps Institution of Oceanography, La Jolla, California*

(Manuscript received 15 June 2010, in final form 13 October 2010)

### ABSTRACT

Ocean wave energy is used to drive a buoyant instrument platform down a wire suspended from a surface float. At the lower terminus of the profiling range, the cam that rectifies wave vertical motion is released and the package, termed the Wirewalker, free ascends. No electronic components are used in the profiler, and only a few moving parts are involved. The Wirewalker is tolerant of a broad range of payloads: the ballast is adjusted by adding discrete foam blocks. The Wirewalker profiles 1000–3000 km month<sup>-1</sup>, vertically, with typical missions lasting from days to months. A description of the profiler is presented along with a discussion of basic profiling dynamics.

### 1. Introduction

The Wirewalker (WW) is a vertically profiling instrument package propelled by ocean waves. In its simplest form, it is a means of attaching any internally recording instrument to a wire suspended from the sea surface. The WW's profiling extends the one-dimensional time series recording of the instrument to a two-dimensional depth–time record. The elements of the WW system include a surface buoy, a wire suspended from the buoy, a weight at the end of the wire, and the profiler itself. The wire and weight follow the surface motion of the buoy. The wave-induced motion of the water is reduced with increasing depth, and the relative motion between the wire and the water is used to propel the WW profiler (see Fig. 1). A cam mechanism on the profiler engages the suspension wire as it descends and releases it as it ascends. The profiler is thus pulled downward, with the maximum downward force determined by the combined mass of the wire below the profiler and the weight at the end of the wire.

At the bottom of the wire, the WW hits a mechanical stop that causes the cam to remain open. The profiler then floats toward the surface, reaching a terminal velocity set by its buoyancy and drag. It is effectively decoupled from the vertical motion of the surface, enabling extremely

precise sampling. At the top of the profile, the cam is reset and the WW ratchets downward. In moderate sea states the WW profiles downward at 10–20 m min<sup>-1</sup>, and round-trip with an ascent rate of ~0.5 m s<sup>-1</sup>, as set by its buoyancy and drag. In typical deployments, the WW travels vertically roughly 1000 km month<sup>-1</sup>. Systems with a negatively buoyant profiler can also be created. These are pulled upward by the waves and released at the surface, achieving a smooth descent.

Relative to buoyancy-driven vehicles, such as profiling floats and gliders, the WW is extremely simple. The ballasting of the profiler requires much less precision. Buoyancy is adjusted simply by adding foam blocks to the structure. Given the weight tolerance, a variety of internally recording instruments can be bolted on the WW frame, ballasted approximately, and deployed. The Wirewalker can be anchored in coastal settings, tethered to deep-sea moorings, or allowed to drift freely. Vertical profiles of velocity, as well as scalar quantities, can be obtained if the WW mooring is anchored or navigated.

Even though the Wirewalker has been evolving for over a decade (Rainville and Pinkel 2001) the approach is far from new. In 1945, John Isaacs built a “sea sled” that rectified the horizontal motion of shoaling waves (Behrman and Isaacs 1992, 168–169). He used the sled to haul instruments and gear offshore through the surf zone. In the 1970s Isaacs and colleagues explored a variety of wave-powered devices, including a “wave pump” that worked on the identical principle as the WW, except in reverse (Isaacs et al. 1976; Wick and Castel 1978). Rather than propelling a vehicle downward, the pump

---

*Corresponding author address:* Dr. Robert Pinkel, Mail Code 0213, Office 356 OAR, 9500 Gilman Drive, Scripps Institution of Oceanography, La Jolla, CA 92093-0213.  
E-mail: rpinkel@ucsd.edu

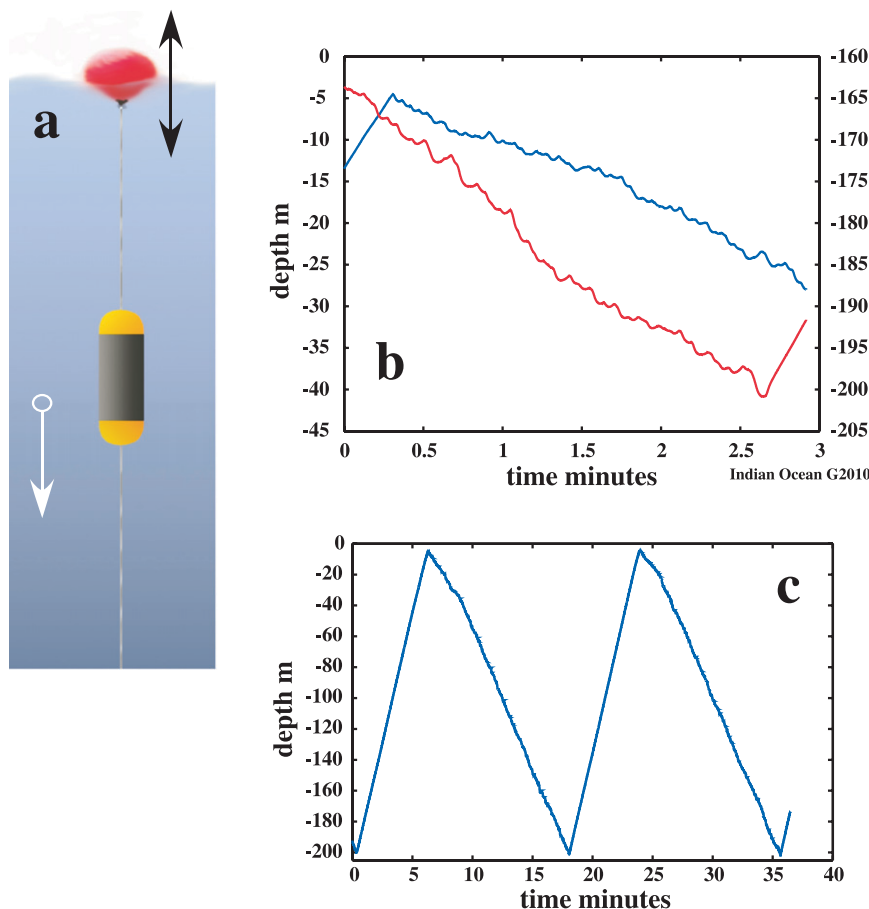


FIG. 1. (a) A schematic of the Wirewalker vertically profiling system. Vertical motion of the surface float is transferred to the weighted deployment wire and rectified by a cam in the profiler. (b) The profiler ratchets downward irregularly: slowly (blue) near the surface, and more rapidly (red, scale at right) at depth. Note that higher-frequency motions dominate the near-surface descent, while lower-frequency waves contribute more at depth. In spite of the oscillatory nature of the forcing, the profiler is almost always traveling downward. Wave groupiness has a clear affect on the descent rate. (c) The ascent proceeds at the upward terminal velocity of the profiler, which is substantially decoupled from surface motion.

brought nutrient-rich water from depths as great as 100 m to the surface. In the 1990s, the Seahorse vertical profiler was developed at the Bedford Institute of Oceanography (Hamilton et al. 1999). With a fully programmable profiling trajectory, the Seahorse is a high-tech predecessor of the Wirewalker.

For operation under the arctic ice, Morison (Eckert et al. 1989) developed a profiler that “flies” vertically along a wire, with lift generated by the relative motion between the ice pack and the upper ocean. Delicate ballasting was necessary to enable operation in low-current conditions. The overall compressibility of the profiler was matched to seawater to further enhance performance. A modern variant, the “Wireflyer,” is currently being developed by D. Hebert (2010, personal communication) at the University of Rhode Island.

With access to wave power one can achieve sampling densities well beyond those attained by most battery-powered vehicles. For example, a profiler deployed in 15-m water off Imperial Beach, California, cycled over forty thousand times during a 6-week deployment in fall 2009. A Seabird SBE49 CTD, an Eco-triplet particle-scattering instrument, and a fluorometer were profiled. Operating in parallel, an offshore instrument tracked the vertical evolution of the temperature field (Fig. 2), documenting the shoaling internal tide, among other signals. The WW design challenge is to tap the power of the wave field without allowing that power to destroy key system components.

Here we describe our current Wirewalker, a descendant of the design described in Rainville and Pinkel (2001; see also Fig. 3d). Profiler mechanical assembly is described

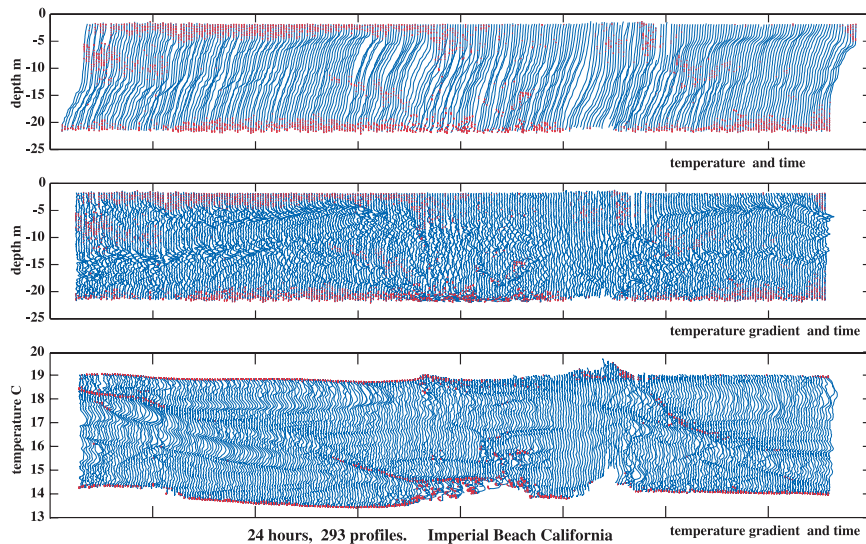


FIG. 2. (top) A 24-h temperature–pressure record obtained off Imperial Beach, CA, by M. Omand. Deployed in 25-m depth, the WW profiled 293 cycles in the course of the day. The profiling time, roughly 5 min, varied by  $\sim 10\%$  because of the changing wave conditions. Sections of the profile where colder water overlies warmer water (red dots) are shown. (middle) When the temperature gradient is plotted vs time, the systematic evolution of the strain field is seen. (bottom) When the temperature gradient is plotted vs temperature, the gross effect of vertical advection is removed. Intense overturning (inversion activity) is seen in the upper and lower boundary layers. It is also associated with the convective instability of semidiurnal internal waves with downward phase propagation.

first, followed by an idealized study of the dynamics of wave-powered vertical profiling.

## 2. The Wirewalker profiler

The initial Wirewalker was a drag-based device, designed to be “fixed” to the local water, just as the deployment wire is fixed to the surface. It became apparent that this is a suboptimal approach for these profilers (J. Pompa 2005, personal communication). The design has transitioned to a much more streamlined aspect ratio (Fig. 3). Low drag and large entrained mass are essential to the performance of the present system.

The WW is constructed around an elongated central box that provides good strength and stiffness for its weight. The rectifying cam is installed at the center of the box, and guide rollers for the wire are fixed at each end. The box, cam, and roller assemblies can be opened quickly, so that the deployment wire can be laid in and then contained. Prototype designs that required that the wire be threaded in from one end proved to be operationally awkward. Blocks of flotation foam can be added to the central box to render the basic WW neutrally buoyant.

Given that the WW typically costs less than the instruments that it hauls, and weighs less than the batteries

that are hauled, it is critical that the payload be firmly attached to the central core of the instrument. In our present design, standard instrument clamps are attached to rails that are an integral part of the WW central core, Fig. 3c. This modular mounting approach allows instruments, wiring, and batteries to be approximately ballasted in the laboratory, prior to being attached to the WW frame. Access to the instruments and wiring is unobstructed. To protect the payload, split-cylinder crash guards are affixed to the outside of the instrument mounts (Fig. 3a). These lock the mounts into a rigid structure and enable the WW to be dragged over the rail of a small boat or launched in piñata mode from a larger vessel.

Primary structural elements are made from  $\frac{3}{4}$ " polyethylene sheet, with  $\frac{1}{4}$ " polyethylene for the skins of the central box and  $\frac{3}{8}$ " polypropylene for the cylindrical crash guards. Most parts are fabricated on a numerically controlled water-jet cutter. Mechanical assembly of the basic WW takes several hours.

The heart of the WW is the cam mechanism that rectifies the vertical motion of the suspension wire (Fig. 4). The goal is to design a cam that will lock onto and release the wire in response to very small relative displacements. The cam should neither suffer degradation nor degrade the wire over the course of millions of operational cycles.

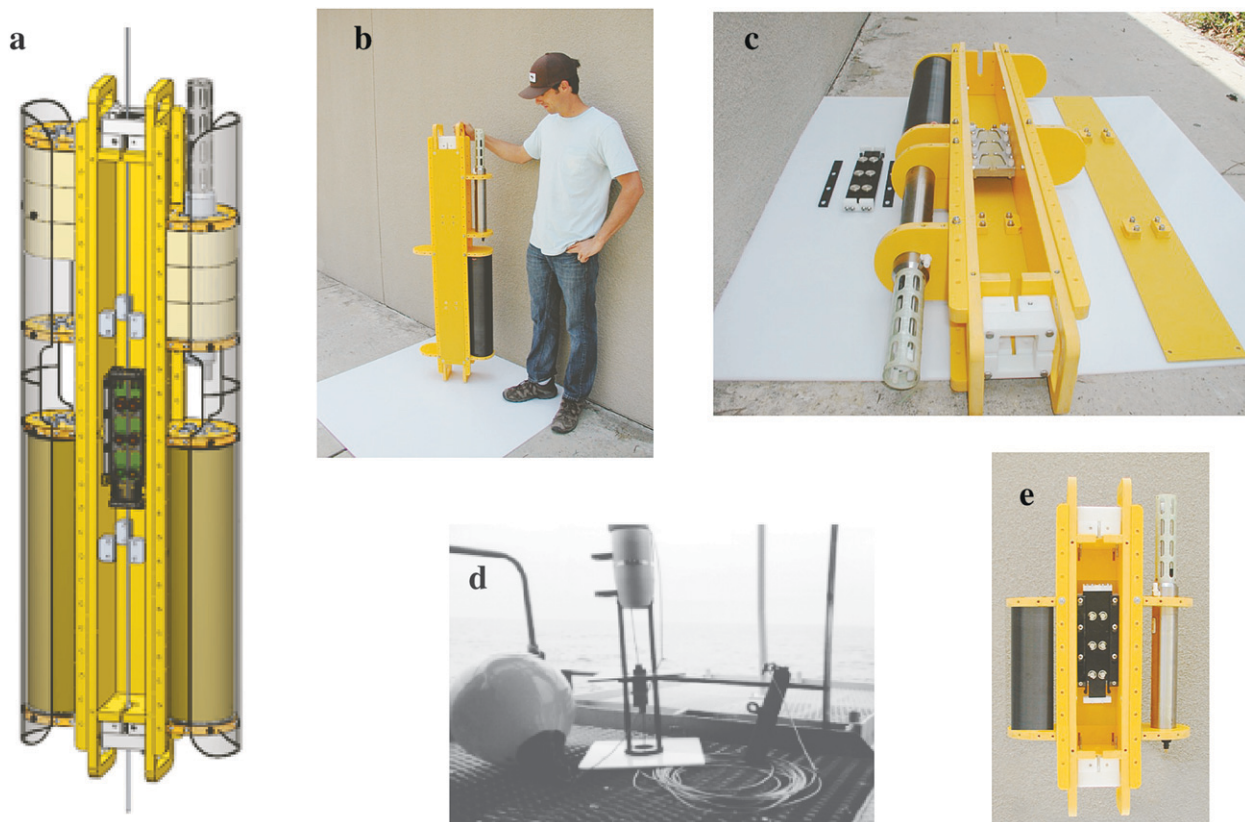


FIG. 3. (a) Schematic of the Wirewalker, showing the cam (black), central core (yellow), floatation (white), and external crash guards (transparent). (b) The full-sized profiler with a SBE49 CTD and battery case attached. The crash guards are removed here. (c) The profiler with the core open and the cam disassembled. (d) The original drag-based WW of Rainville and Pinkel (2001). (e) Schematic of a 0.3-m profiler with an SBE39 TP recorder.

The current cam is a six-wheel pinch-roller design. The central carriage of the cam, containing the wheels, is free to slide vertically relative to its external mount. When descending, the carriage is in its downward position and the wheels can engage the wire whenever there is downward relative motion of the wire. At the bottom of the

profiling range, a “stop” is affixed to the wire. This hits the bottom of the carriage, knocking it upward where it is captured by a retaining snap. In the upward position, the roller wheels are unable to pinch the wire and the WW is free to ascend, uncoupled from wire motion. At the top of the profiling range, a second “stop” is attached to the

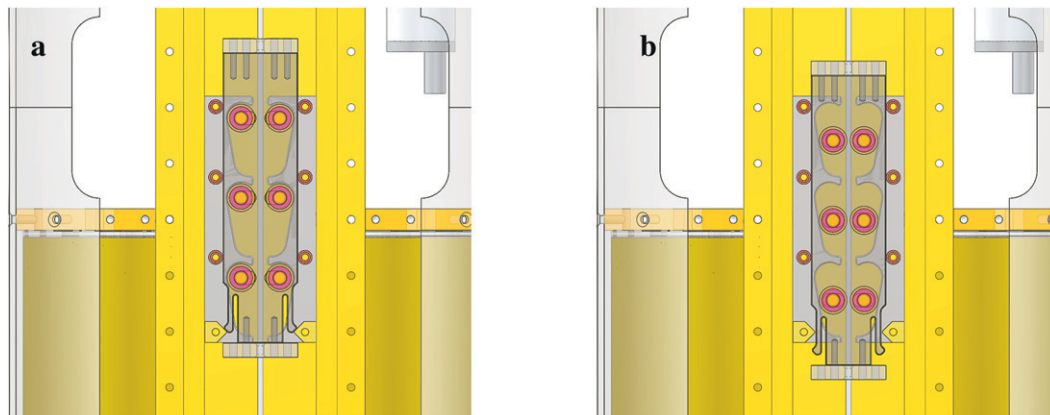


FIG. 4. Schematic of the Wirewalker cam during (a) ascent and (b) descent. See text for description.

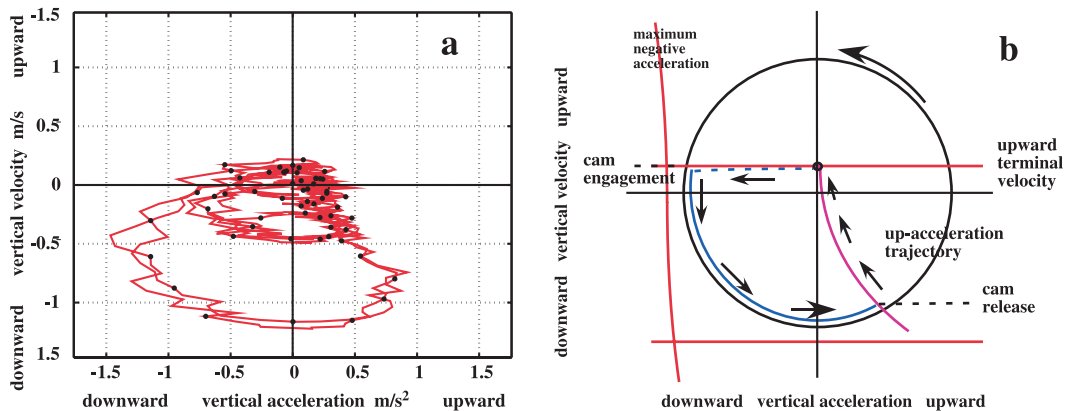


FIG. 5. (a) A representative acceleration–velocity state diagram during descent. Data are obtained from the pressure sensor of an SBE49 CTD, smoothed by 1 s in time. The black dots are spaced at 0.5-s intervals. Multiple successive wave periods are included, with two large-amplitude crests temporally separated by several smaller waves. Independent of wave properties, the upward acceleration trajectories coalesce. Note that the profiler is almost always moving downward while accelerating upward relative to the surrounding water. Maximum acceleration is of order 0.15 g, implying a relatively gentle ride. The “o” indicates the upward terminal velocity, as determined by the rise rate. For a buoyancy of  $10 \text{ kg m s}^{-2}$ , the corresponding  $C_d = 40 \text{ kg ms}^{-2}$ . The “\*” along the upward acceleration trajectory implies an entrained mass of 50 kg (see text). (b) An idealized representation of the diagram for a monochromatic sinusoid (see text).

wire. When contacted, the carriage is sprung from its latched-up position. It descends relative to the fixed frame of the cam and reengages the roller wheels with the wire.

Over the profiling cycle, the greatest impact that the WW encounters is when colliding with the bottom stop. Here the velocity difference between the surface and local depth is the greatest. “Transition shocks” at both the lower and upper limits of the profiling range are cushioned by mounting the stops at the head of a  $\sim 1\text{-m}$  section of rubber hose that surrounds the deployment wire.

The greatest wear on the wire occurs at the top of the cycle, where the cam is reengaged. The actual force on the wire is not large relative to that at greater depth, but the impact occurs repeatedly at the identical spot on the wire.

Using  $3/16''$  galvanized wire for typical deployments, we find that the wire can begin to fail after  $\sim 10\,000$  profiles. The roller wheels require replacement after  $\sim 2000\text{-km}$  vertical travel, depending principally on the entrained mass of the profiler. The cam works equally well on the 3-mm Spectra line. Long-term wear tests on the Spectra have yet to be conducted.

### 3. Wirewalker dynamics

As an entry to WW behavior, it is instructive to plot WW vertical velocity versus vertical acceleration as a “state diagram” (Fig. 5) during the downward, wave-powered segment of the profile. Vertical motion is determined by differentiating the pressure sensor on the

Seabird SBE49 CTD being carried in this 2008 Indian Ocean deployment. Because the surface waves are barotropic, pressure is unchanging in a reference frame moving with the water. The pressure signal thus indicates motion relative to the local water, which is the quantity of importance here.

The equations governing the various phases of the state diagram can be easily integrated, providing a quantitative prediction of WW performance. The governing wave characteristics, Wirewalker, and mooring parameters are listed in the Table 1. For simplicity, the surface buoy is assumed to have infinite buoyancy, such that it follows the motion of the sea surface exactly. Also, non-Archimedean effects<sup>1</sup> are ignored, because the buoyancy of the WW is small compared to the product of its virtual mass and typical wave accelerations.

Considering Fig. 5b, we chose the time when the WW is rising but not accelerating as the “start” of a typical wave cycle. Under the effect of buoyancy, the WW is free ascending near its terminal velocity (in this example) as

<sup>1</sup> Non-Archimedean effects are associated with the motion of bodies in an accelerating fluid caused by the difference in the density of the body relative to the fluid. The best-known effect is seen when an automobile rounds a corner at high speed. Occupants of the car are thrown toward the outside of the turn, while helium balloons carried inside the car are accelerated inward. Isaacs (see Behrman and Isaacs 1992) used this effect to design sea surface buoys that “dodged” big waves, as well as submerged, moving breakwaters that efficiently dissipated wave energy without penetrating the sea surface.

TABLE 1. Definitions.

Quantity	Symbol	Units
Wave amplitude	$A$	m
Wave frequency	$\sigma$	$s^{-1}$
Entrained mass	$M$	Kg
Deployment weight	$m$	Kg
Wire length	$L$	m
Wire weight	$W$	$Kg\ m^{-1}$
Buoyant force	$b$	N
Drag coefficient	$C_d$	$kg\ m^{-1}$

the sea surface rises through its mean position. When the rise rate of the sea surface becomes less than that of the Wirewalker, the cam engages and the WW assumes the motion of the sea surface. Schematically, the WW transitions to near-maximum vertical acceleration very quickly (Fig. 5b), although the smoothed pressure signal (Fig. 5a) shows this as a gradual transition. Maximum downward acceleration is experienced near the wave crest, and power is supplied to the WW during the following quarter cycle. During this period, the motion of the WW is exactly that of the surface float. WW acceleration, velocity, and displacement relative to local water are given from linear wave theory:

$$w_{WW}(t) = w(t) = \sigma A \cos(\sigma t) [1 - e^{-k(\sigma)z}]. \quad (1)$$

$$a_{WW}(t) = a(t) = \sigma^2 A \sin(\sigma t) [1 - e^{-k(\sigma)z}].$$

When the upward acceleration of the wire exceeds the maximum upward acceleration of the WW, as set by its entrained mass, buoyancy, and drag, the cam disengages. Disengagement occurs when

$$a(t) > (b - C_d |w_{WW}| w_{WW}) / M. \quad (2)$$

The WW then follows a fixed trajectory that is independent of sea surface or mooring details. The force balance is given as

$$a_{WW}(t) = (b - C_d |w_{WW}| w_{WW}) / M. \quad (3)$$

Starting with the velocity of the WW as the cam releases, Eq. (3) can be integrated forward in time to yield the trajectory.

The time spent in this phase of the motion cycle is nearly  $3/4$  of the wave period. Highly buoyant or high-drag profilers will quickly arrive at their upward terminal velocity and remain there until the next wave cycle. Massive, streamlined profilers will continue downward through much or all of this period.

Given enough time, the WW will start to float upward, potentially reaching terminal velocity,

$$w_{WW}^+(t) = (b/C_d)^{1/2}, \quad (4)$$

provided that the subsequent wave cycle does not begin. If the bottom stop is encountered, then the cam is released and the profiler ascends at the terminal velocity.

Note that, until this point, the magnitude of the weight at the end of the deployment wire has been unimportant. The surface float extracts energy from the wave field as it lifts the wire and weight in preparation for the next cycle.

Complications arise when either the downward terminal acceleration or terminal velocity limits are exceeded and the WW goes into ‘‘parachute mode.’’ The segment of suspension wire above the profiler becomes slack. These thresholds are affected by the weight of the wire and the deployment weight at the end of the wire:

$$a_{Max}(t) = \{b - C_d |w_{WW}| w_{WW} - [m + W(z + L)]g\} / [M + m + W(z + L)], \quad (5)$$

$$w_{WW} = -(\{-b + [m + W(z + L)]g\} / C_d)^{1/2}. \quad (6)$$

The acceleration threshold is most likely exceeded shortly after the cam is engaged, while the velocity threshold becomes important toward the end of the power cycle.

If either threshold is exceeded, one can integrate forward in time to obtain the depth–time trajectory. When the depth of the WW exceeds the depth of the surface float relative to the local water, the wire goes taut and the cam opens.

Changing wave frequency affects the acceleration–velocity ellipticity of the state diagram. Changing wave amplitude sets the area contained by the trajectory, as well as the time spent on the ‘‘coasting downward’’ versus ‘‘floating upward’’ portions of the upward acceleration trajectory. The difference between sea surface and deep motion grows as  $(1 - e^{kz})$ , where  $k$  is the wavenumber of the wave and  $z$  is positive upward. High-wavenumber (frequency) waves are instrumental in allowing the WW to travel downward from the immediate sea surface. Energy from ever-longer waves is available as profiler depth increases. Profiler speed increases with increasing distance from the surface (Fig. 1b).

Representative profiler trajectories and trade-offs are given in Figs. 6–8 for monochromatic wave forcing. Of the performance-governing WW parameters listed in Table 1, all are easy to determine. It is necessary to know the buoyancy of the entire package, which can be determined by pulling the ballasted WW downward in

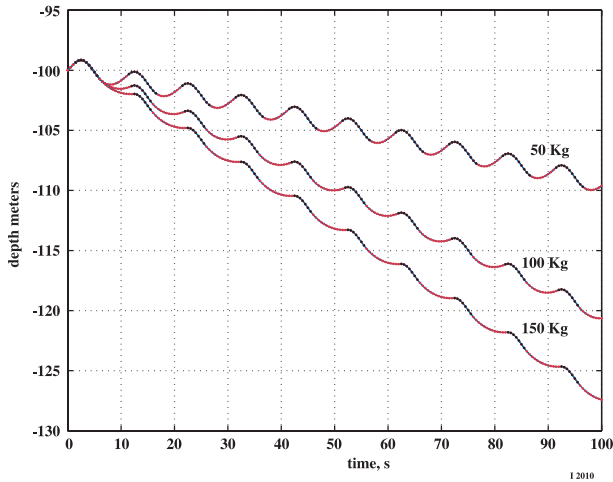


FIG. 6. Wirewalker descent trajectories for a system with 1-kg positive buoyancy, driven by a 10-s wave with 1-m amplitude. As entrained mass is increased from 50 to 150 kg, performance improves. The fraction of each cycle where the cam is engaged is indicated (black). The increase in mass enables the WW to coast downward during the period that the cam is disengaged. The low-inertia profiler (top curve) starts to ascend almost immediately after cam release.

a small laboratory test tank and measuring the force required. With this information,  $C_d$  can be determined by the free-ascent rate. Then,  $M$  can be obtained from the upward acceleration curve following cam release

during descent. If desired, a downward drag coefficient can be determined directly, by adding a known weight to the WW and allowing it to sink to its downward terminal velocity. To estimate the downward terminal acceleration and velocity thresholds, the mass of the deployment weight and the wire must also be known.

The transition from an inertial (coasting) to a drag-based (Fig. 3d) profiler is set by the dimensionless metric  $M/(C_d A)$ . As wave amplitude grows, drag forces increase faster than inertial. For  $M < 30$  Kg and  $C_d > 50$  Kg  $m^{-1}$ , profiler performance increases with increasing drag (Fig. 7). The increase is more apparent for larger waves ( $A = 2.5$  m; Fig. 7a) than for smaller ( $A = 1$  m; Fig. 7b). Performance is always improved by increasing entrained mass.

#### 4. Wirewalker deployment

An attractive aspect of the WW is the ease of deployment, with a yacht fender (Fig. 3d) being a suitable surface float. For high-value payloads and more complex systems (Fig. 9a), a more secure mooring system has been developed (Fig. 9b). The idealized mooring of Fig. 1a is augmented such that the surface buoy is fitted with a GPS receiver, Iridium modem, and a strobe light. The float is designed to have a large phase response to high-frequency waves. The phase shift, neglected in the

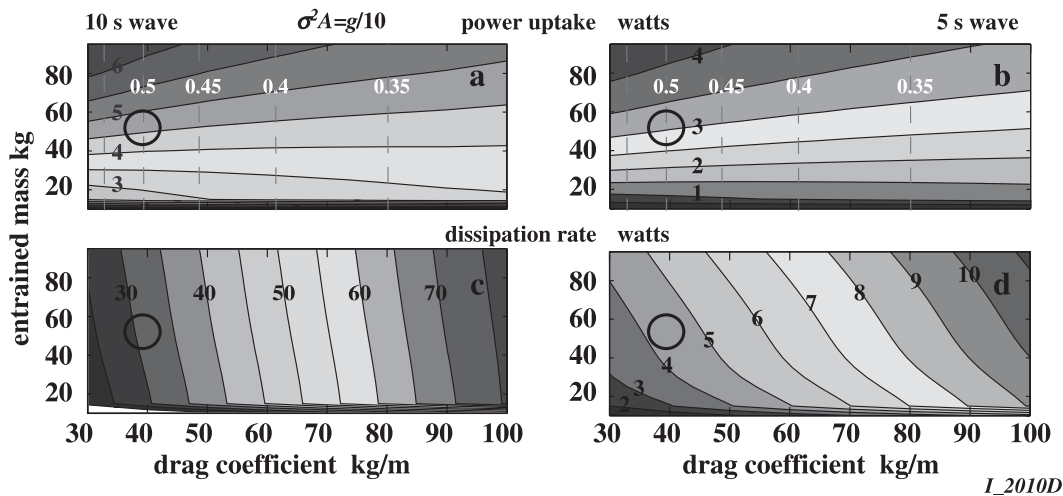
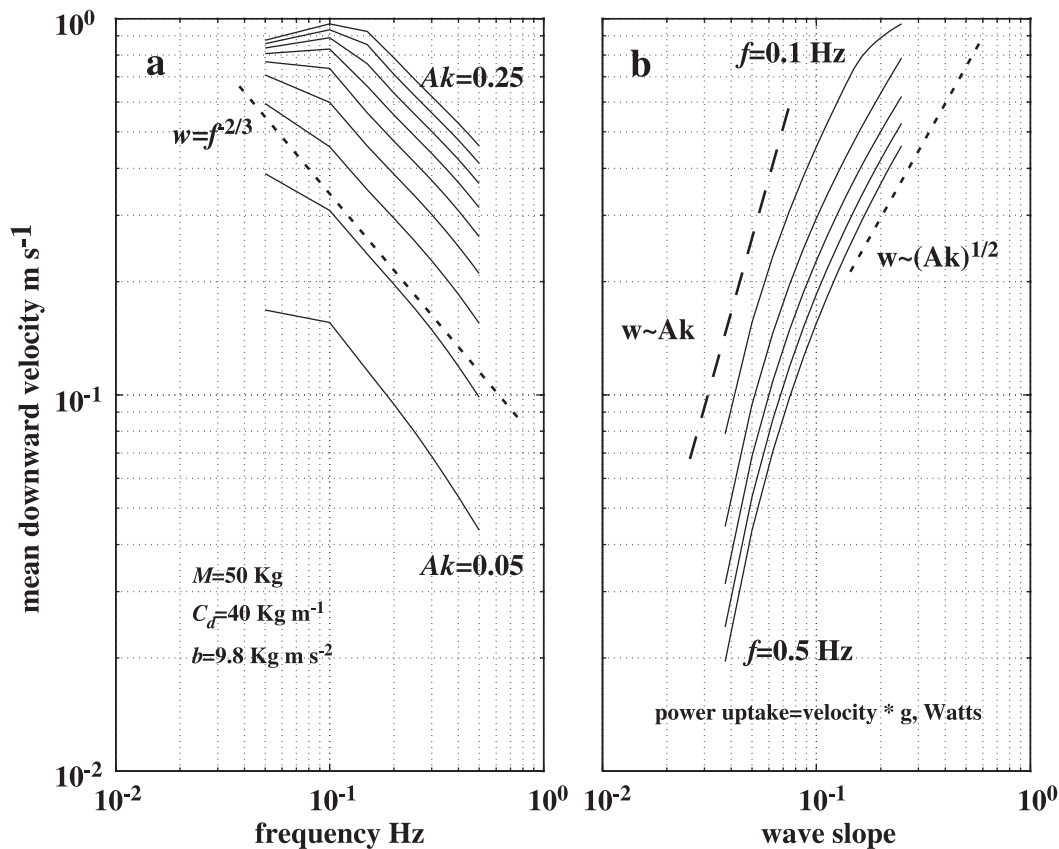


FIG. 7. Modeled profiler performance for a WW of 9.8 kg  $m s^{-2}$  buoyancy at a depth of 100 m, being forced by monochromatic waves of a (a),(c) 10- and (b),(d) 5-s period. Wave amplitudes are 2.5 and 0.6 m, corresponding to maximum wave acceleration of 0.1 g and a maximum slope of 0.1. The open circle indicates the operating region of the Indian Ocean WW of Figs. 3 and 5. (a), (b) Power uptake is the rate of gain of WW potential energy  $P = b\langle w \rangle$ . It generally increases with increasing entrained mass and decreasing drag. The exception is at low mass, where the WW transitions from inertial- to drag-based operation. For this example, with  $b = g$  kg  $m s^{-2}$ , the mean vertical velocity is just  $P/g \sim (0.3-0.4)$  m  $s^{-1}$ . Realized speeds (Fig. 1b) are closer to 0.25 m  $s^{-1}$ . (c), (d) The WW dissipates more energy than it gains. For the same downward average velocity, more power is dissipated by the 10-s forcing because peak velocities are larger.



12010E

FIG. 8. (a) The WW descent rate as a function of frequency for waves of slope 0.05–0.25 for the WW modeled above at a depth of 100 m. (b) Descent rate as a function of wave slope at frequencies of 0.1–0.5 Hz.

previous idealized discussion, is very effective in driving the WW down from the immediate surface, even in calm conditions. The surface float must be ballasted such that it remains upright even if the deployment wire breaks.

Otherwise, communications with the float will be lost and there will be no record of the failure mode. A section of chain and a swivel connect the 3/16" galvanized deployment wire to the float.

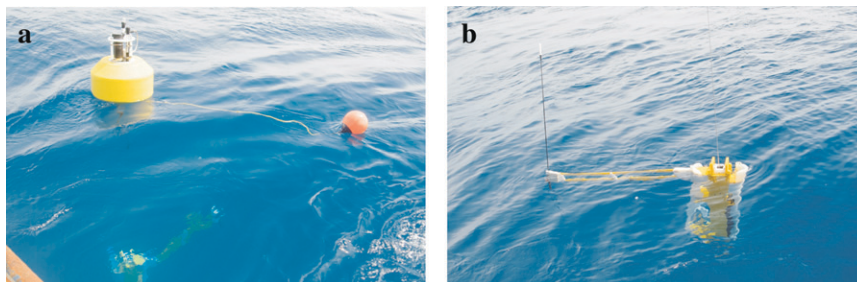


FIG. 9. (a) A ~1-m-diameter foam surface float with a steel subframe is presently used to suspend the WW in open-ocean experiments. Batteries, a 950-MHz line-of-sight radio link or Iridium modem, and a strobe are housed in the float. The small auxiliary float (orange) aids in recovery. The WW is surfacing in the lower left of the figure. (b) A WW equipped with a Digi point-to-point radio link. Data are collected and formatted aboard the WW by a Persitor CF2 processor. The pressure case housing the electronics is also used to package instrument batteries. Data are transferred to the surface float when the WW is at the surface. The flexible antenna arm folds alongside the profiler when the device is being deployed.

The “stops” that strike the cam carriage and initiate reversal of the profiler are small sections of reinforced neoprene hose. These cushion the impact at each end of the profile. The bottom weight is sized to assure that the maximum downward acceleration and velocity limits [Eqs. (5) and (6)] are seldom exceeded, given the mass and drag of the profiler.

To anchor in coastal water, a negatively buoyant tether line is attached from the deployment weight to a seafloor chain and anchor. When practical, this tether is made long enough that the mooring can be recovered by grappling the tether and raising the anchor first. With a buoy-first recovery, the recovery vessel is effectively anchored by the mooring as the hardware is brought aboard.

For mooring in the deep sea, a promising approach is to tether the profiler float to a traditional surface mooring. Extended deep-sea moored deployments have yet to be attempted. Deep-sea, free-drifting deployments are the forte of the WW.

## 5. Operational experience

Prototype Wirewalker systems have been deployed off southern California, Rhode Island, Virginia, and Texas, in the North Pacific and Indian Oceans, as well as the South China Sea. To date, the WW has hauled CTDs, optical particle counters, fluorometers, and various current meters. When measuring currents, a small rudder on the WW body is sufficient to control profiler orientation. Because quality data are collected during ascent, at upward speeds of  $(0.24\text{--}0.5) \text{ m s}^{-1}$ , the orientation of the incoming flow to the current meter is approximately constant. Instruments can be mounted such that wakes from the sensor housing or the profiler itself are avoided. Given the smooth ascent rate, the WW is an attractive platform for upper-ocean current measurement.<sup>2</sup>

The performance model presented here assumes that the surface buoy follows the sea surface displacement perfectly. In fact, the drag of the buoy-wire system, and its resonance with (typically) high-frequency waves, serve to introduce relative motion between the buoy and the surface. These second-order effects greatly improve the ability of the WW to descend from just below the surface.

System phase is altered as the WW extracts power from the wave field. It is often possible to determine whether the WW is ascending or descending based on the observed motion of the surface float in a seaway. A more advanced model of WW dynamics is in preparation.

---

<sup>2</sup> Even during descent, the WW velocity acceleration trajectory is gentler than of a fixed-depth sensor on a conventional surface mooring (Fig. 5b, bounding circle).

In moored applications, profiling can be interrupted by strong currents and by fouling, a problem common to all moorings. The vertical motion of the WW deployment wire can saw through kelp strands and other large seaweed in several hours. These encounters are easily monitored in profiler performance records. Fouling by commercial fishing gear is often a concern.

Large currents can stretch a mooring laterally, such that the WW deployment wire is not vertical. We have had instances where profiling was curtailed as the WW attempted to descend into the face of the currents. The present “inertial based” profilers are much more effective at penetrating a current than the earlier drag-based devices. Increasing the deployment weight and reducing drag help to improve high-current performance.

The principal mechanical weakness in the present system is at the upper limit of the deployment wire. At the initiation of descent, the cam compresses the deployment wire at exactly the same spot on each profile, just below the upper “stop.” Subsequent “grabs” occur randomly along the length of the wire. After  $\sim 10^4$  profiles the wire begins to show significant wear. This is a concern when a 20-m section of the ocean is being profiled and  $10^4$  profiles can be collected in a month. For 200-m deployments, wire life approaches a year, and battery capacity becomes the limiting factor.

The WW enables a simple instrument to do the work of many, turning one-dimensional time series data into a two-dimensional depth–time record. To do so, the instrument must sample continuously during ascent. If the scientific need is for one sample every 15 min, a traditionally moored instrument might spend most of its undersea time “turned off.” Using a WW, profiling would be repeated every  $\sim 15$  min, but the sensor would be on  $\sim 50\%$  of the time. Thus, while the WW needs to haul only a single instrument, it must also haul the batteries of a large fraction of the instruments that it replaces.

Given the weight of the batteries and the cost of the pressure cases needed to house them, electrical power is a significant issue. While battery capacity is improving and lower power instruments are being designed, there is also motivation for using wave power to generate electricity onboard.

A variant of the Wirewalker is now being produced by Brooke Ocean Technology.

*Acknowledgments.* The authors thank Luc Rainville, Jon Pompa, Achintya Madduri, Jody Klymak, Jennifer MacKinnon, Andrew Lucas, and Melissa Omand for assistance with the development and operation of the Wirewalker. The Imperial Beach data were graciously provided by M. Omand and R. Guza. Support for

Wirewalker development was provided by Grants NSF OCE05-01783 and ONR N00014-08-1-1022.

## REFERENCES

- Behrman, D., and J. D. Isaacs, 1992: *John Isaacs and His Oceans*. Special Publications, Amer. Geophys. Union, 230 pp.
- Eckert, A. C., J. H. Morison, G. B. White, and E. W. Geller, 1989: The autonomous ocean profiler: A current driven oceanographic sensor platform. *IEEE J. Oceanic Eng.*, **14**, 195–202.
- Hamilton, J., G. Fowler, and B. Beanlands, 1999: Long-term monitoring with a moored wave-powered profiler. *Sea Technol.*, **40**, 68–69.
- Isaacs, J. D., D. Castel, and G. L. Wick, 1976: Utilization of energy in ocean waves. *Ocean Eng.*, **3**, 175–187.
- Rainville, L., and R. Pinkel, 2001: Wirewalker: An autonomous wave-powered vertical profiler. *J. Atmos. Oceanic Technol.*, **18**, 1048–1051.
- Wick, G., and D. Castel, 1978: The Isaacs wave-energy pump: Field tests off the coast of Kaneohe Bay, Hawaii: November 1976–March 1977. *Ocean Eng.*, **5**, 235–242.